IOP Publishing | Astro Ltd
Laser Physics Letters
Laser Phys. Lett. **11** (2014) 115902 (5pp)
doi:10.1088/1612-2011/11/11/115902

Circular split-ring core resonators used in nanoscale metal–insulator–metal band-stop filters

Huiyun Zhang, Duanlong Shen and Yuping Zhang

Qingdao Key Laboratory of Terahertz Technology, College of Electronic Communication and Physics, Shandong University of Science and Technology, Qingdao 266510, People's Republic of China

E-mail: ypzhang1976@126.com

Received 23 February 2014, revised 9 August 2014
Accepted for publication 11 September 2014
Published 1 October 2014

Abstract

A novel structure with a circular split-ring core is presented to improve the surface plasmon polaritons' (SPPs) transmission characteristic through a nanoscale band-stop filter of the metal–insulator–metal (MIM) structure. With a metal wall created at the center of the disk resonator, novel structures and the transmission characteristics are studied in several different situations. Some absorption peaks appear in the spectrum, and will shift while changing the dimension of the gap and the refractive index of the insulator. The magnetic field distributions with SPPs propagating through the filter are plotted. Meanwhile, a method is adopted to enhance the absorption peak values of the transmittance. This is important for potential applications in optical integrated circuits and other nanoscale devices.

Keywords: surface plasmon polaritons, nanoscale filter, circular split-ring core resonator, transmission characteristic

(Some figures may appear in colour only in the online journal)

1. Introduction

Surface plasmon polaritons (SPPs) are electromagnetic modes on the metal surface area formed by the interaction of free electrons and photons. SPPs have been used in some of the latest studies and new types of optical circuits and devices. Relations between SPPs, resonant modes, and surface local field were studied, and optical fields were enhanced by rough-surface-induced field superpositon [1]. A strong optical nonlinear effect was studied at the nanoscale in aluminum, and a new effective third-harmonic generation for nano slits made in aluminum and gold [2]. Recently, several kinds of plasmonic filter constructed by metal–insulator–metal (MIM) configuration have received much attention due to the simple structures and excellent filtration, and because some waveguides can be constructed with regular geometric structure used as band-pass [3–8] and band-stop [9–13] filters. Hosseini *et al* have investigated a plasmonic filter with a rectangular ring resonator, which prevents some specific wavelengths from passing through the structure [14–18]. Split-ring resonators have been designed which play the role of the band-stop filter [10, 12]. A two-dimensional plasmonic structure constructed by two MIM straight waveguides and a ring resonator has been investigated by Wang *et al* [3]. There are several specific wavelengths which pass through the structure, and the peak values of transmittance could move towards the long-wavelength direction when the radius of the ring is increased. Band-pass filters with rectangular MIM waveguides have also been proposed [4, 7]. It was found that the transmission peaks could be modulated by changing the resonator's cavity length, and the magnitude of transmittance could be tuned by varying the distance between the straight waveguides and the resonator.

In this letter, a band-stop plasmonic filter with a circular split-ring core resonator is proposed. A metal wall of the circular split-ring with a gap is created at the center of the disk resonator, with a finite-difference time-domain (FDTD) method used to simulate the transmission characteristics of the filter in different cases. Band-stop filters with disk resonators [8, 13, 16] and closed ring [12, 15] resonators have been studied with filter characteristics through varying the refractive index of the medium, the size of the resonators, the distance between the bus waveguide and the resonator, and so on. With

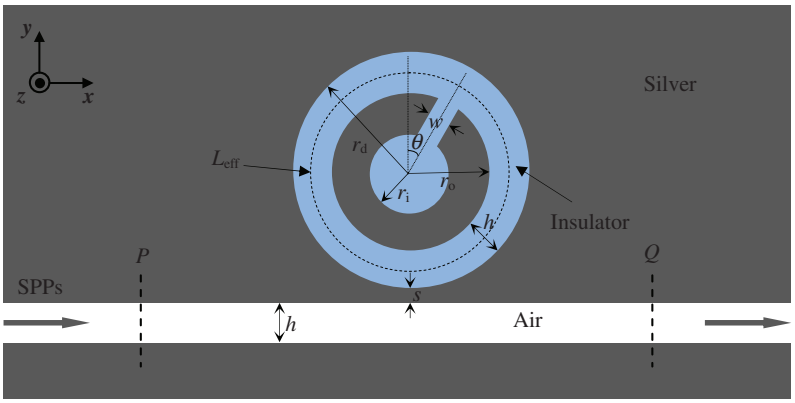

Figure 1. The structure of the nanoscale MIM filter with a metal split-ring core resonator.

the circular split-ring core proposed in this letter, the filters can be tuned in more active methods based on the core. The resonant strength of the absorption peaks can be enhanced by changing the positions of the gap properly. By varying the width of the gap and the refractive index of the medium, the absorption spectrum can be tuned in wider ranges.

2. Theory and model

The 2D nanoscale structure is shown in figure 1. The gray part is silver; the blue part is the insulator which is set to be air or another dielectric; and the bus waveguide is filled with air. If the insulator could be replaced by some noble gases, high energy photoelectrons could be generated by plasmonic enhanced near-fields in it [19]. A silver split-ring is positioned at the center of the medium disk. The width of the gap is w. θ is the angle between the radial direction of the gap and the original direction. The width of the bus waveguide h is set to be 50 nm which is much smaller than wavelengths. Transverse magnetic (TM) SPP modes are supported to propagate along the x direction. The distance between the resonator and the bus waveguide s is 10 nm. r_d (=150 nm), r_o (=100 nm) and r_i (=50 nm) are the radiuses of the medium disk, the outer radius of the split-ring and the inner radius of the split-ring, respectively. Two power monitors are set at P and Q to detect the incident power P_{in} and the transmitted power P_{out}, with the transmittance defined as $T = P_{out}/P_{in}$.

The dispersion relation of SPPs is expressed by the following equation:

$$\tanh\left(\frac{h}{2}k_0\sqrt{n_{eff}{}^2-\varepsilon_0}\right)=-\frac{\varepsilon_0\sqrt{n_{eff}{}^2-\varepsilon_m}}{\varepsilon_m\sqrt{n_{eff}{}^2-\varepsilon_0}} \tag{1}$$

where $n_{eff} = \beta/k_0$ is the effective refraction index of SPPs, β and k_0 are the propagation constants of SPPs and free space, respectively, ε_0 is the permittivity of air and ε_m is that of the metal's. Consider the Lorentz model [20]: take only the first term of the summation and neglect the other terms, then ω_a equals 0. The model can then be expressed by the following Drude model:

$$\varepsilon_m(\omega)=\varepsilon_\infty-\frac{\omega_p{}^2}{\omega^2+i\omega\omega_c}. \tag{2}$$

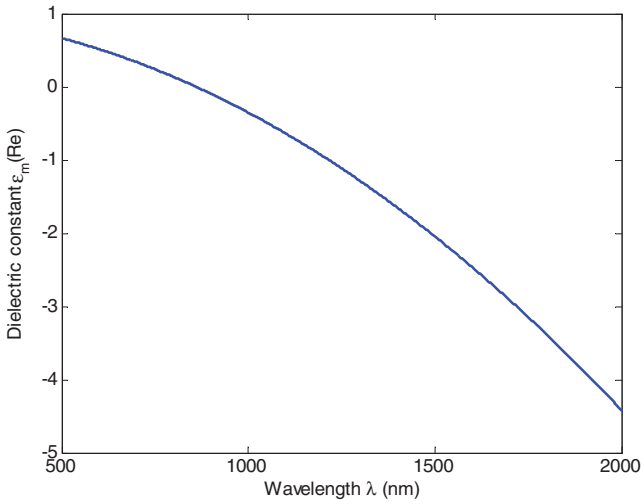

Figure 2. Dependence of Re(ε_m) of silver on the wavelength of incident light in the cases of the Drude model.

Separating the real and imaginary part, it can also be expressed as:

$$\varepsilon_m(\omega)=\varepsilon_\infty-\frac{\omega_p{}^2}{\omega^2+\omega_c{}^2}+i\frac{\omega_p{}^2\omega_c}{\omega^3+\omega_c{}^2\omega}. \tag{3}$$

Here, $\varepsilon_\infty = 1$, $\omega_c = 27.3$ THz, $\omega_p = 2196.3$ THz. The permittivity spectrum of the Drude model is plotted in figure 2. The Drude model adopted in this paper can be regarded as a simplified form of the Lorentz model and is clearer in describing actual metal.

In the simulations, the grid size along x and y directions are chosen to be $\Delta x = \Delta y = 5$ nm and the time step is $\Delta t = \Delta x/2c$; here c is the velocity of light in the vacuum. The computational space is surrounded by open boundary conditions of impedance matching absorption in the x direction and periodic boundary conditions in the y and z directions.

When SPPs propagate through the bus waveguide, the resonance effect will occur and obvious absorption peaks will be achieved accordingly. The resonant wavelength is determined by the resonance condition:

$$L_{eff}n_{eff}=N\lambda,(N=1,2,3...). \tag{4}$$

Here, L_{eff} is the effective length of the resonator; n_{eff} is the effective refraction index of SPPs.

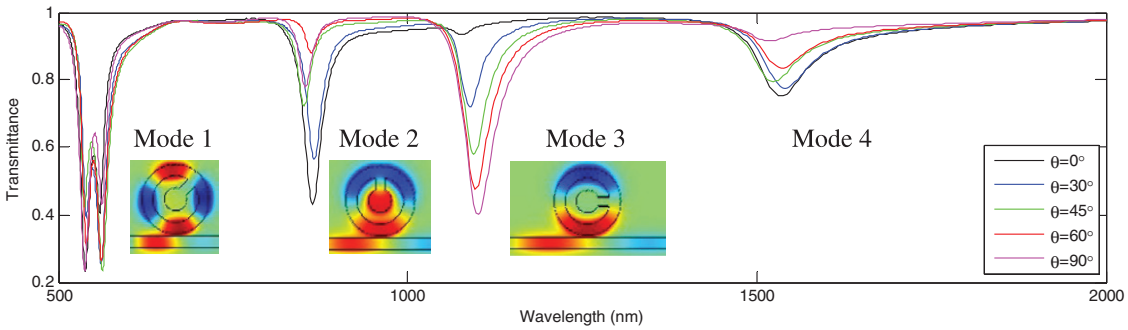

Figure 3. The transmission properties with different directions of the gap.

3. Simulations and results

The transmission properties with different directions of the gap and magnetic field patterns of H_z at the peak values in different θ are shown in figure 3. The insulator is set to be air; the width of the gap is 40 nm; and the angle θ is chosen to be 0°, 30°, 45°, 60° and 90°, respectively. It can be seen in figure 3 that the resonant absorption will be strong at the wavelengths 562.85 nm with $\theta = 45°$, 864.55 nm with $\theta = 0°$ and 1100.92 nm with $\theta = 90°$; these are defined as mode 1, mode 2 and mode 3. Mode 4 can be neglected owing to its weak absorption. These directions can be called 'effective directions'. The generation of the magnetic field patterns implies that circulating currents are formed in the metal ring. Resonances are supported with these patterns, and the field patterns are diverse in different angles based on different symmetries. The degeneracy of the resonances appeared due to symmetry reduction. For one direction of the gap, one kind of the degenerating mode is excited, and the mode possessing an asymmetric field pattern based on the symmetry axis is excited. For other directions, the modes with corresponding resonance wavelengths are also excited, with the absorption strengths selectively enhanced or weakened. In the actual application, the resonant wavelengths can be enhanced selectively with different directions of the gap. In order to illustrate the effective directions, the peak values of transmittance depend on θ as plotted in figure 4.

From the description of figure 4, mode 1 has an ideal transmission characteristic at all the gap directions. The effective direction of the mode 2 is 0° and that of mode 3 is 90°, which is the same as that mentioned in figure 3.

As equation (4) shows, the effective length of the resonator and the refractive index of the insulator can affect the transmission characteristics of the nano filter. So the resonant wavelengths can be controlled by changing the refractive index n with constant effective length L_{eff}. Thus active devices, such as tunable filters or optical switches, can be designed. The refractive index n can be changed by heating, electro-optic effect (including Pockels effect and Kerr effect), acousto-optic effect, and so on. The bus waveguide is filled with air all of the time, and the resonator with the insulator of the varied refractive index in this case. Similar to formula (1), the dispersion relationship can be expressed by the following form in this case:

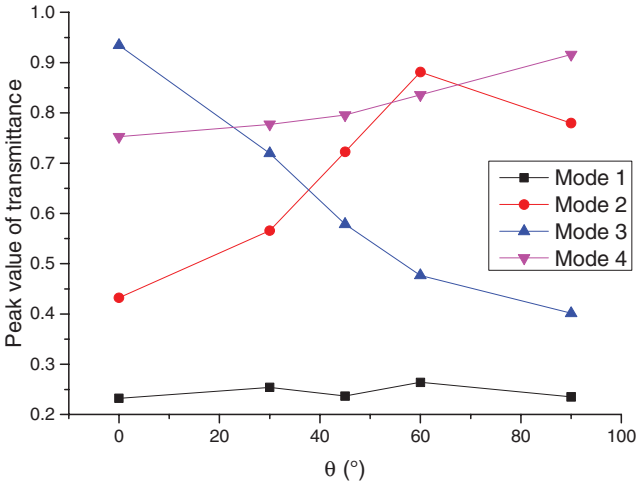

Figure 4. Peak values of the transmittance as a function of the direction angle θ of the gap.

$$\tanh\left(\frac{h}{2}k_0\sqrt{{n_{\text{eff}}}^2-\varepsilon_d}\right) = -\frac{\varepsilon_d\sqrt{{n_{\text{eff}}}^2-\varepsilon_m}}{\varepsilon_m\sqrt{{n_{\text{eff}}}^2-\varepsilon_d}}. \quad (5)$$

Here ε_d is the permittivity of the insulator, and the refractive index n is set to be 1.0, 1.2, 1.4, 1.6, 1.8 and 2.0. The transmittance spectrums are plotted in figure 5(a), with the spectrum shift being observed clearly. The modes of the transmittance exhibit shift with n increased. The resonant wavelength dependent of the refractive index of the insulator is plotted in figure 5(b). In this case, mode 2 and mode 4 are neglected due to their weak resonances.

From figure 5, the resonant wavelengths of the spectrum shift towards the long-wavelength direction (red shift) with the refractive index n increased from 1.0 to 2.0, and the shift range is wide for tuning.

A mode split (another style of spectrum shift) can be achieved by varying the width of the gap, as is shown in figure 6. The transmittance spectrum is shown in figure 6(a), and the resonant wavelengths of mode 1, mode 2 and mode 3 as a function of the gap width w is plotted in figure 6(b). The varied gap of the resonator will affect the equivalent capacitance in the equivalent circuit of the structure, thus the equivalent impedance can be changed accordingly. The current in the circuit can be affected by the varied impedance and the

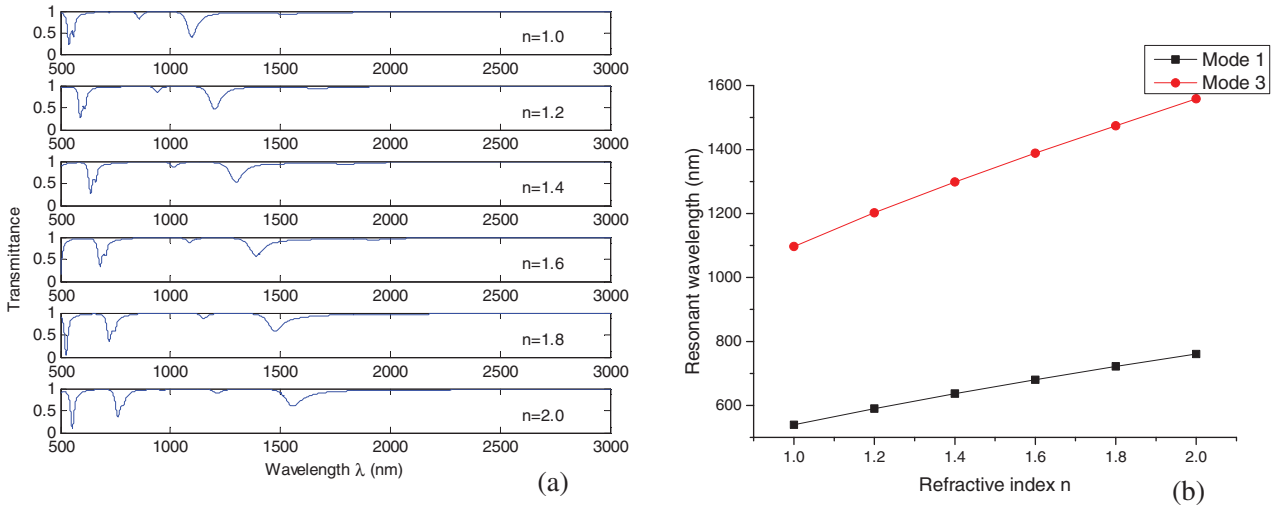

Figure 5. (*a*) The transmittance of the filter with different refractive indexes n at the direction of $\theta = 90°$. (*b*) The resonant wavelengths of mode 1 and mode 3 as a function of n.

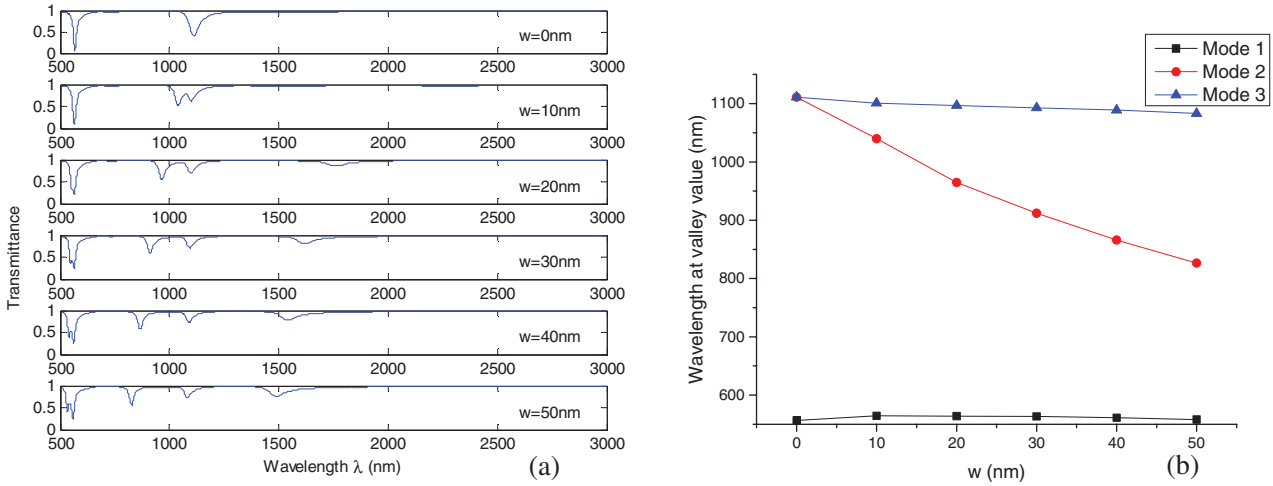

Figure 6. (*a*) The transmittance spectrum with varied width of the gap in the case of $\theta = 30°$. (*b*) The resonant wavelengths of mode 1, mode 2 and mode 3 dependent of the width w.

electromagnetic fields which associate with the transmission characteristics will be changed simultaneously. The width of the gap is varied from 0 to 50 nm in the case of $\theta = 30°$.

It can be seen from figure 6 that mode 2 can be split off from mode 1 while increasing the width w from 0 nm, which is called blue shift due to its moving to the short-wavelength direction. Actually, the mode split phenomenon is essentially a specific spectrum shift. If the width of the gap can be broadened continuously from 50 nm, the blue shift range will be wider.

4. Conclusion

In conclusion, a novel MIM filter structure by creating a circular split-ring core has been put forward to improve the SPPs' transmission character, and the resonant modes of SPPs in the resonator have been simulated by the FDTD method. By varying the position of the gap, the strength of the resonance is enhanced. Spectrum shift can be controlled by changing the refractive index of the insulator and the size of the gap. Mode split as a specific spectrum shift can also be observed.

Acknowledgments

This work is supported by the National Natural Science Foundation of China (Grant No. 61001018), Natural Science Foundation of Shandong Province, China (Grant No. ZR2011FM009, ZR2012FM011), the Research Fund of Shandong University of Science and Technology (SDUST), China (Grant No. 2010KYJQ103), SDUST Research Fund (Grant No. 2012KYTD103), Qingdao innovative leading talent plan (13-CX-25), project of Shandong Province Higher Educational Science and Technology Program (Grant No. J11LG20), Qingdao Economic & Technical Development Zone Science & Technology Project (Grant No. 2013-1-64)

References

[1] Zhang F, Chen P, Li X, Liu J T, Lin L and Fan Z W 2013 *Laser Phys. Lett.* **10** 045901
[2] Melentiev P N, Konstantinova T V, Afanasiev A E, Kuzin A A, Baturin A S, Tausenev A V, Konyaschenko A V and Balykin V I 2013 *Laser Phys. Lett.* **10** 075901
[3] Min C J and Veronis G 2009 *Opt. Express* **17** 10757
[4] Wang B and Wang G P 2004 *Opt. Lett.* **29** 1992
[5] Han Z H, Liu L and Forsberg E 2006 *Opt. Commun.* **259** 690
[6] Wang T B, Wen X W, Yin C P and Wang H Z 2009 *Opt. Express* **17** 24096
[7] Okamoto H, Yamaguchi K, Haraguchi M and Okamoto T 2010 *J. Nonlinear Opt. Phys.* **19** 583
[8] Wang G X, Lu H, Liu X M, Gong Y K and Wang L R 2011 *Appl. Opt.* **50** 5287
[9] Zentgraf T, Liu Y M, Mikkelsen M H, Valentine J and Zhang X 2011 *Nature Nanotechnol.* **6** 151
[10] Liu L, Han Z H and He S L 2005 *Opt. Express* **13** 6645
[11] Dionne J A, Sweatlock L A, Atwater H A and Polman A 2006 *Phys. Rev.* B **73** 035407
[12] Zheng G G, Su W, Chen Y Y, Zhang C Y, Lai M and Liu Y Z 2012 *J. Opt.* **14** 055001
[13] Tao J, Wang Q J and Huang X G 2011 *Plasmonics* **6** 753
[14] Hosseini A and Massoud Y 2007 *Appl. Phys. Lett.* **90** 181102
[15] Peng X, Li H J, Wu C N, Cao G T and Liu Z M 2013 *Opt. Commun.* **294** 368
[16] Yun B F, Hu G H and Cui Y P 2013 *Plasmonics* **8** 267
[17] Zand I, Mahigir A, Pakizeh T and Abrishamian M S 2012 *Opt. Express* **20** 7516
[18] Zand I, Abrishamian M S and Berini P 2013 *Opt. Express* **21** 79
[19] Ciappina M F, Shaaran T, Guichard R, Pérez-Hernández J A, Roso L, Arnold M, Siegel T, Zaïr A and Lewenstein M 2013 *Laser Phys. Lett.* **10** 105302
[20] Rakić A D, Djurišić A B, Elazar J M and Majewski M L 1998 *Appl. Opt.* **37** 5271